



Research Progress on Enhanced Oil Recovery by CO₂ Flooding in Low Permeability Reservoirs

Wei Zhou¹, Meng-yao Niu², Wan-jing Luo²(✉), and Xiao-tong Liu¹

¹ PetroChina Jidong Oilfield Company, Tangshan, China

² School of Energy Resources, China University of Geosciences, Beijing, China
luowanjing@cugb.edu.cn

Abstract. Summarized the current development situation of low permeability oil reservoirs at home and abroad, and sorted out the development process of three stages: indoor research, pilot testing, and field application of CO₂ flooding at home and abroad. The micro oil displacement mechanism in the CO₂ oil displacement process was systematically elaborated, and some widely used calculation methods for the minimum miscibility pressure (MMP) of CO₂ and crude oil were summarized, providing a theoretical basis for significantly improving oil recovery. On the basis of tracking and researching the on-site application and effectiveness of CO₂ flooding technology for improving oil recovery in 33 low permeability reservoirs both domestically and internationally, 5 rock properties and 2 fluid properties of reservoirs using CO₂ flooding method were summarized, and the impact of 2 displacement modes and 5 injection methods on CO₂ flooding efficiency was analyzed. The research results indicate that the displacement method of the miscible flooding and the injection method of periodic gas injection have better CO₂ oil displacement effect. Provide on-site application reference and experience support for the efficient application of CO₂ flooding technology to improve oil recovery in low permeability reservoirs in China.

Keywords: Low-Permeability Reservoirs · Enhanced Oil Recovery · CO₂ Flooding

Copyright 2023, IFEDC Organizing Committee.

This paper was prepared for presentation at the 2023 International Field Exploration and Development Conference in Wuhan, China, 20–22 September 2023.

This paper was selected for presentation by the IFEDC Committee following review of information contained in an abstract submitted by the author(s). Contents of the paper, as presented, have not been reviewed by the IFEDC Technical Team and are subject to correction by the author(s). The material does not necessarily reflect any position of the IFEDC Technical Committee its members. Papers presented at the Conference are subject to publication review by Professional Team of IFEDC Technical Committee. Electronic reproduction, distribution, or storage of any part of this paper for commercial purposes without the written consent of IFEDC Organizing Committee is prohibited. Permission to reproduce in print is restricted to an abstract of not more than 300 words; illustrations may not be copied. The abstract must contain conspicuous acknowledgment of IFEDC. Contact email: paper@ifedc.org.

© The Author(s), under exclusive license to Springer Nature Singapore Pte Ltd. 2024
J. Lin (Ed.): IFEDC 2023, SSGG, pp. 343–366, 2024.
https://doi.org/10.1007/978-981-97-0268-8_28

1 Introduction

As exploration and development of onshore oil fields continue, techniques for enhancing oil recovery in low-permeability reservoirs have become a focus of attention [1]. Both domestically and internationally, low-permeability oil reserves are abundant, with recoverable reserves reaching 483×10^8 t [2]. In China, low-permeability oil and gas resources account for 49% of the total oil and gas resources, making it a strategic area for oil resource replacement [3, 4]. However, due to poor pore-permeability conditions and strong reservoir heterogeneity, the development of low-permeability oil reservoirs is challenging, with the current overall recovery rate only around 18% [1, 5].

During the tertiary oil recovery process, the use of carbon dioxide to enhance oil recovery (CO₂-EOR) has been applied in oil fields for over 40 years and has become a relatively mature tertiary oil recovery development method [6]. CO₂-EOR not only promotes an increase in oil field production but also utilizes and sequesters CO₂ resources, reducing greenhouse gas emissions. In September 2020, China clearly stated its goal of striving to reach peak CO₂ emissions by 2030 and achieving carbon neutrality by 2060. In recent years, China's CO₂ emissions have been increasing year by year, with CO₂ emissions reaching 119×10^8 t in 2021, accounting for 33% of the world's total CO₂ emissions. The use of CO₂ flooding in low-permeability reservoirs can achieve the dual purpose of enhancing oil recovery and geological sequestration, achieving both environmental and economic benefits [6, 7].

The United States first applied water containing carbonate to the K&S project in northeastern Oklahoma in 1958, marking the beginning of the field application of CO₂-EOR. In 1964, the first pure CO₂ miscible flooding project was implemented in the Mead Strawn oil field in Texas. Nine years later, in 1972, the first CO₂-EOR commercial project in the world was put into production in the SACROC block of the Kelly-Snyder oil field in Texas. This project established the CO₂ water-gas alternating drive displacement method, which initially increased the average production rate of a single well by more than three times. Its success marked the beginning of the maturity of CO₂ flooding technology. From 1980 to 1992, in response to the oil crisis, the United States introduced a series of policies to stimulate the enthusiasm of oil companies and private capital, promoting the rapid development of CO₂-EOR technology. During this period, the number of CO₂-EOR projects increased to 54, with annual EOR production increasing to 783×10^4 t. By 2014, the United States had a total of 137 CO₂-EOR projects, with an annual EOR production of 1371×10^4 t [8, 9].

China began researching CO₂-EOR in the late 1960s, initially conducting indoor research and pilot trials in small test areas in the Daqing oil field, but research into injection was largely suspended due to CO₂ source limitations [10]. After 2000, the discovery of CO₂-containing natural gas reservoirs in the Songliao Basin enabled CO₂-EOR research in Jilin and Daqing oil fields. The Yushulin oil field in Daqing conducted oil displacement experiments using CO₂, and as of 2022, the cumulative increased oil amount reached 11×10^4 t. In 2005, the CO₂ huff-n-puff enhanced oil recovery (EOR) field test was initiated in Caoshe oilfield, and the huff-n-puff was achieved in 2008. By the end of 2020, the cumulative oil production increment was 13.52×10^4 t. In 2017, the CO₂ flooding EOR field test was conducted in the Huang 3 area of Changqing oilfield. By the end of 2018, the effective good ratio corresponding to the well network reached 56.5%

in just one year, and the cumulative oil production increment was 748.1 t, indicating a good EOR effect. In September 2020, with the proposal of the “dual carbon” target, CO₂-EOR ushered in a rapid development opportunity. By the end of 2021, CO₂-EOR experimental areas of different types, such as Daqing low permeability, Jilin ultra-low permeability, and Changqing super-low permeability, had been established [11]. CO₂-EOR experiments are blooming everywhere, and major oil companies and oilfields are exploring this technology [12].

2 CO₂ EOR Mechanism

The critical temperature of CO₂ is 31.1 °C, and the corresponding critical pressure is 7.495 MPa. CO₂ fluid above the critical temperature and critical pressure are in a supercritical state [13]. When CO₂ reaches a supercritical state, its density is similar to that of liquid, and its viscosity is similar to that of gas, but its diffusion coefficient is nearly 100 times that of liquid [14]. In addition, CO₂ is more soluble in water than hydrocarbon gases, and its solubility in crude oil is greater than that in water, indicating strong solubilization [13]. The physical and chemical properties of CO₂ determine its displacement mechanism in the EOR process, which mainly includes changing the rock properties of the reservoir, altering the fluid properties of the reservoir, dissolving gas drive, and huff-n-puff effect [15].

2.1 Changing Rock Properties of Reservoir

Physical Properties: The chemical reaction $\text{CO}_2 + \text{H}_2\text{O} \rightarrow \text{H}_2\text{CO}_3$ indicates that CO₂ injected into the reservoir reacts with formation water to generate carbonic acid, and the hydrogen ions produced by the ionization of carbonic acid decrease the pH value of the formation fluid, making it acidic. The acidic fluid reacts with the rock and its cementation materials, thereby dissolving rock minerals, and increasing porosity and permeability [15–17]. However, this process is also accompanied by the precipitation of new minerals and the transport of debris particles. When the actual well spacing is large, the mineral components dissolved near the injection well may precipitate near the production well with the decrease of pressure, thereby reducing the permeability of the reservoir [15].

Wettability: After CO₂ is injected into the reservoir and dissolved in water, it corrodes upon contact with the rock surface, enhancing the hydrophilicity of the rock. On the other hand, CO₂ dissolved in crude oil produces asphaltene precipitation, and polar substances such as asphaltenes adsorb on the surface of rock particles, causing the wettability of the rock to shift toward oil-wet [15].

2.2 Altering Fluid Properties of Reservoir

Expansion: After CO₂ is injected into the reservoir and dissolved in crude oil, the volume of the oil expands, and its internal kinetic energy increases, making it separate from the confinement of the formation water and rock surface to become movable oil. At the

same time, the elastic energy of the formation increases, enhancing the efficiency of oil displacement [15–19].

Reduction of viscosity: CO₂ dissolved in crude oil disperses in a supercritical state, reducing the interaction forces between hydrocarbon molecules and lowering the viscosity of the crude oil, thereby significantly enhancing its flowability. The higher the original viscosity of the crude oil, the higher the percentage of viscosity reduction under the action of carbon dioxide [15–19].

Molecular diffusion: CO₂ gas enters the formation water and crude oil through slow dissolution and diffusion of molecules, thereby increasing the volume of the crude oil, reducing its viscosity, and improving the oil displacement efficiency. At the same time, after CO₂ is dissolved into the crude oil, sufficient single-phase diffusion can slow down the gas channeling of CO₂ and increase the spreading coefficient. Therefore, during CO₂ flooding, it is necessary to appropriately reduce the injection rate to ensure that the gas molecules fully diffuse in the oil phase, thereby obtaining the best oil recovery efficiency [15, 17].

Improvement of water-oil mobility ratio: After CO₂ is dissolved in the formation water and crude oil, they are carbonated separately. After the formation water is carbonated, its viscosity increases by more than 20%, and its mobility decreases; after the crude oil is carbonated, its viscosity decreases, and its mobility increases. The mobility of water and oil tends to be closer, improving the water-oil mobility ratio, expanding the sweep area, and improving the oil displacement efficiency [15].

Reduction of oil-water interfacial tension: During CO₂ flooding, CO₂ can mix with light hydrocarbons in crude oil, reducing the interfacial tension between the oil and water phases, thereby reducing the resistance during CO₂ displacement and ultimately increasing the oil recovery rate. The greater the CO₂ concentration, the more significant the reduction in interfacial tension [15–19].

Extraction and vaporization: Supercritical CO₂, due to its strong solubility and high fluidity, is often used as an extractant. Supercritical CO₂ can effectively extract and vaporize light hydrocarbons in crude oil, especially residual oil that has been expanded but not yet released from the constraints of the formation water, and undergoes interphase mass transfer with CO₂ gas. As the extraction and vaporization deepen, CO₂ approaches or reaches a state of miscibility with the crude oil, and the interfacial tension drops significantly, thereby significantly improving the displacement efficiency [15–19].

2.3 Gas Dissolution Drive

During the oil displacement process, CO₂ is dissolved in the crude oil. When the reservoir pressure drops, the dissolved CO₂ separates from the oil and forms bubbles. As the pressure drops further, the CO₂ gas expands, producing elastic expansion energy that promotes the flow of crude oil into the wellbore. This is the gas dissolution drive effect [15–19].

2.4 Miscible Effect

During CO₂ flooding, when the pressure reaches the miscibility pressure, the CO₂ and crude oil undergo multiple contacts, resulting in the evaporation or extraction of light

hydrocarbons from the crude oil. This causes the injected gas at the front of the gas flood to mix with the crude oil, forming a miscible zone, as shown in Fig. 1. The advancement of the miscible zone can effectively displace oil, and the oil recovery can reach more than 90% in some cases [15]. CO₂ flooding can be classified into two types based on whether CO₂ and crude oil reach miscibility: CO₂ immiscible flooding and CO₂ miscible flooding [18].

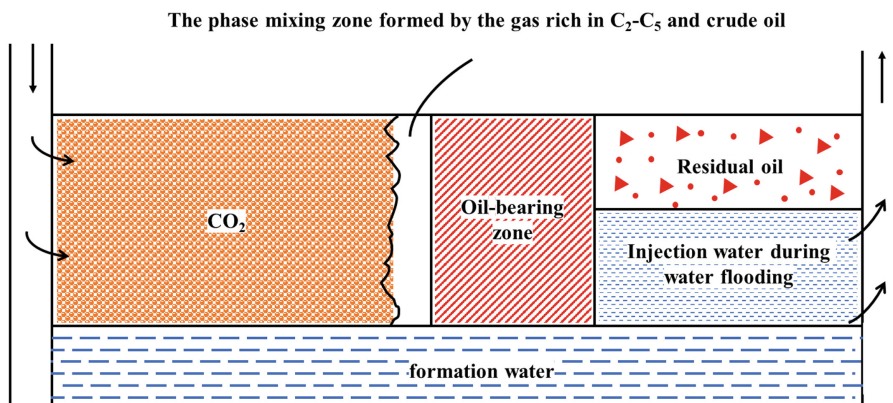


Fig. 1. Schematic diagram of CO₂ and crude oil multiple contacts miscible flooding

(1) CO₂ non-miscible displacement

In the CO₂ non-miscible displacement process, the pressure of the formation is lower than the minimum miscible pressure between CO₂ and crude oil, resulting in a clear interface between the two and making it difficult for them to mix. In this mode of oil recovery, only a portion of the CO₂ dissolves in the crude oil, causing the volume of the crude oil to expand and the viscosity to decrease, thereby achieving the purpose of oil displacement. However, since only a portion of the CO₂ interacts with the crude oil, the displacement efficiency is low and issues such as rapid breakthrough of CO₂ gas can easily occur. Therefore, this method has limited application in the field and its maturity level is much lower than that of the miscible displacement mode. However, after years of research and exploration, effective monitoring techniques for CO₂ injection, methods for removing blockages in the injection formation and production profile, and effective selection of suitable reservoirs for CO₂ non-miscible displacement have been developed. Therefore, in recent years, CO₂ non-miscible displacement technology has been revived [8].

(2) CO₂ miscible displacement

When the formation pressure is greater than the minimum miscible pressure between CO₂ and crude oil, but less than the formation's fracturing pressure, CO₂ and crude oil mix to achieve CO₂ miscible displacement. After CO₂ and crude oil are mixed, they dissolve in each other without a clear interface, eliminating interfacial tension and

greatly improving displacement efficiency. Since CO₂ miscible displacement has a better effect on increasing the recovery rate than non-miscible and near-miscible displacement, most oilfield experiments and developments at home and abroad use CO₂ miscible displacement mode. For oilfields where the original formation conditions cannot achieve miscibility, the minimum miscible pressure can be reduced or the formation pressure can be rapidly increased to improve the degree of miscibility. For example, “CO₂ flooding” technology can be used to lower the minimum miscible pressure by enhancing CO₂’s ability to dissolve in crude oil and extract light hydrocarbons from crude oil while injecting large amounts of liquid CO₂ into the local well group through rapid pressure buildup to improve the degree of miscibility [7].

3 Calculation Methods for Minimum Miscibility Pressure (MMP)

One of the key issues in achieving CO₂ miscible flooding technology is determining the minimum miscibility pressure (MMP) for CO₂ flooding. Many experts at home and abroad have researched this, and currently, the methods for determining MMP mainly include experimental methods, empirical formula methods, equation of state methods, and numerical simulation methods.

3.1 Experimental Method

(1) Capillary tube experiment

Among the traditional laboratory methods for determining MMP, the capillary tube experiment is currently the most accurate and reproducible method. Due to its direct and reliable method, it has become a standard method for determining MMP at home and abroad.

The experimental process of the capillary tube experiment is shown in Fig. 2. The capillary tube is a long metal tube filled with sand, glass beads, or other particles inside. The experiment requires saturating the capillary tube with crude oil at the desired temperature and pressure and using a backpressure valve to control the experimental pressure. After the system reaches equilibrium, CO₂ displacement experiment begins. When using this method to determine MMP, CO₂ injection is usually performed at different pressure conditions, and the oil recovery rate when injecting 1.2 times the pore volume of CO₂ is recorded. The oil recovery rate-pressure curve is established, and the inflection point of the curve when the recovery rate is about 90% is defined as the MMP [20–22].

Although the capillary tube experiment is currently considered the most reliable laboratory method for determining MMP, the standard for the length, diameter, and internal filling of the experimental device has not been determined yet. Due to the inability to simulate factors such as viscosity fingering and gravity override and the long experimental time required, the capillary tube experiment has certain limitations.

(2) Bubble Rising Apparatus Method

The experimental apparatus of the bubble-rising method is shown in Fig. 3. The core device of the experiment is the glass tube mounted vertically on the high-pressure

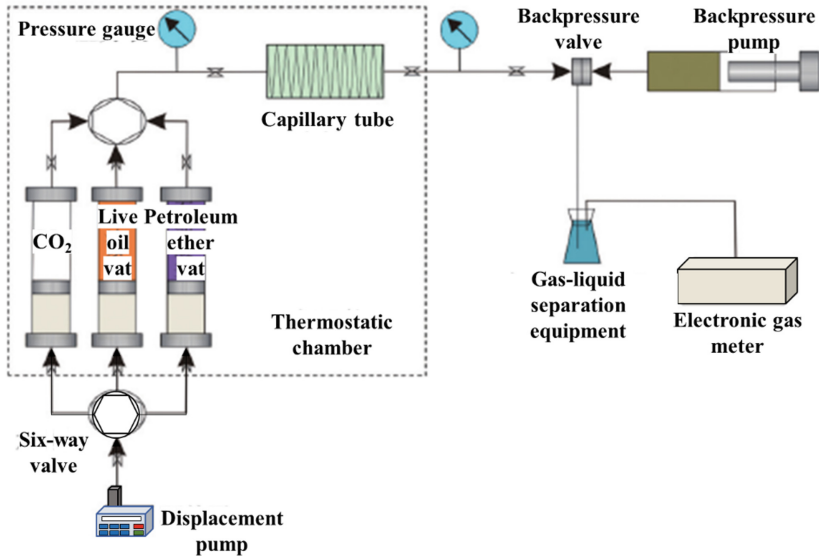


Fig. 2. Schematic diagram of the device for the slim-tube experiment method

observation gauge in the temperature-controlled bath. In the experiment, the CO₂-oil miscible state can be directly observed through the glass tube. At the beginning of the experiment, the glass tube is filled with crude oil and CO₂ gas is slowly injected into the glass tube at different pressure conditions. The changes during the CO₂ bubble rising process are observed and photographed. In the glass tube, the gas-liquid mass transfer occurs at the interface between the CO₂ bubble and crude oil. At low pressure conditions, due to the larger interfacial tension, the bubble shape is larger. As the pressure increases, the interfacial tension decreases, and the bubble becomes smaller. When the interfacial tension is extremely low and the bubble shape is extremely small, it can be considered that the CO₂ and crude oil have reached miscibility [20, 23].

Although the bubble-rising method is very fast, with the experiment taking about 1 h to complete, the results obtained do not have a quantitative standard and are greatly influenced by human factors, leading to large errors. The reliability of the experimental results needs to be verified.

(3) Interfacial Tension Disappearance Method

The interfacial tension disappearance method determines the MMP of CO₂ and reservoir crude oil by directly measuring the interfacial tension between them and using extrapolation [20, 22–24]. Generally, the methods for measuring interfacial tension between gas and liquid include the ring detachment method, pendant drop method, sessile drop method, capillary rise method, and drop volume method. The pendant drop method is usually used in high-pressure systems [23].

The pendant drop method determines the interfacial tension between the two phases by measuring the shape parameters of the liquid droplet suspended at the top of a capillary

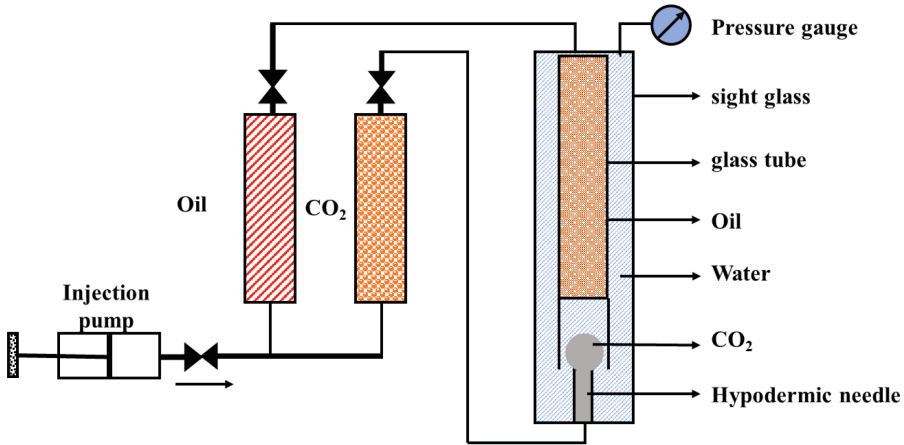


Fig. 3. Schematic diagram of the device for the bubble rising apparatus method

probe. The principle can be expressed as:

$$\gamma = \frac{gD_e^2 \Delta\rho}{H} \quad (1)$$

where γ is the interfacial tension between gas and liquid, N/m; D_e is the diameter of the widest part of the droplet, m; g is the acceleration due to gravity, m/s^2 ; $\Delta\rho$ is the density difference between the gas and liquid phases, kg/m^3 ; and H is the corrected shape factor [24].

The interfacial tension at different pressures can be measured using the pendant drop method. However, since the interfacial tension measuring device cannot measure the pressure at which the interfacial tension becomes zero at the point of phase mixing, the MMP can be calculated by combining the experimental results with the extrapolation method. Compared with the capillary tube method, this method can quickly and simply determine the MMP. However, it has limitations because it cannot account for the impact of porous media on the measurement results [20, 23].

3.2 Empirical Formula Method

Due to its simple and rapid calculation, the empirical formula method has become increasingly favored by researchers. Currently, there are more than 20 published empirical formulas for determining MMP. Below, some of them are selected for introduction.

(1) Yelling and Metcalfe formula [25]

In 1980, Yelling and Metcalfe extrapolated the CO_2 vapor pressure curve to the MMP and predicted CO_2 flooding MMP based on reservoir temperature. At the same time, the Petroleum Institute for Studies in Recovery of Oil (PRI) also proposed a similar empirical formula.

Yelling and Metcalfe formula:

$$P_{mm} = -[1.5832 + 0.19038(1.8T + 32) - 0.00031986(1.8T + 32)^2] \quad (2)$$

Petroleum Institute for Studies in Recovery of Oil (PRI) formula:

$$P_{mm} = -[-4.8913 + 0.0415(1.8T + 32) - 0.0015974(1.8T + 32)^2] \quad (3)$$

(2) Glaso formula [26]

Glaso added the consideration of the effect of intermediate components in crude oil on the minimum miscibility pressure of CO₂ based on the prediction chart made by Benham and others. Two relationship formulas were given based on the content of intermediate components (mol %) in crude oil as a limit:

① When the mole percentage of intermediate components in crude oil is less than 18%:

$$P_{mm} = 20.3214 - 0.0235M_{c7+} + [1.6673 \times 10^{-9} M_{c7+}^{3.73} \exp 786.8M_{c7+}^{(-1.0582)}](0.0127T + 0.225) - 0.8356f_{RF} \quad (4)$$

② When the mole percentage of intermediate components in crude oil is greater than 18%:

$$P_{mm} = 5.5805 - 0.0235M_{c7+} + [1.6673 \times 10^{-9} M_{c7+}^{3.73} \exp 786.8M_{c7+}^{(-1.0582)}](0.0127T + 0.225) \quad (5)$$

where M_{c7+} is the molecular weight of C_{7+} in the dewaxing oil, and f_{RF} is the mole content of C_2 - C_6 in the reservoir fluid.

(3) Alston formula [27]

Alston and others proposed a method to predict the MMP of a gas-containing oil system that reaches miscible displacement through multiple contacts with pure or impure CO₂ gas.

① Pure CO₂ displacement:

$$P_{mm}^{pure} = 8.78 \times 10^{-4} (T_R)^{1.06} (M_{C_{5+}})^{1.78} \left(\frac{x_{vol}}{x_{int}}\right)^{0.136} \quad (6)$$

where T_R is the reservoir temperature, °F, $M_{C_{5+}}$ is the molar mass above C_{5+} , g/mol, X_{vol} is the mole number of volatile components (such as N₂ and C₁) in crude oil, and X_{int} is the mole number of intermediate hydrocarbon components (C₂₋₄, CO₂, and H₂S) in crude oil.

② Impure CO₂ displacement:

$$P_{mm} = 8.78 \times 10^{-4} T^{1.06} (M_{C_5^+})^{1.78} \left(\frac{x_{vol}}{x_{int}}\right)^{0.136} \left(\frac{87.8}{T_{cm}}\right)^{170/T_{cm}} \quad (7)$$

$$T_{cm} = \sum_{i=1}^n W_i T_{ci} - 459.7 \quad (8)$$

where W_i is the weight fraction of component I, T_{cm} is the average critical temperature of the injected gas, °F, T_i is the critical temperature (Rankine temperature R) of component I, °R, and X_{vol} and X_{int} are the mole numbers of the volatile components and intermediate hydrocarbon components in crude oil, respectively.

(4) Silva Formula [28, 29]

Detailed composition analysis of the CO₂-rich phase and oil-rich phase formed by the mixture of CO₂ and crude oil shows that the distribution of molecular sizes in crude oil has a much greater impact on MMP than the changes in hydrocarbon structure. Silva used this to establish a formula for MMP as a function of the molecular weight distribution of crude oil.

First, based on the analysis of the gas phase, normalized weight fractions $W_{iC_{2+}}$ of each fraction of C₂–C₃₁ hydrocarbons (excluding non-hydrocarbons such as C₁, N₂, CO₂, and H₂S) are given:

$$W_{iC_{2+}} = \frac{W_i}{\sum_2^{31} W_i} \quad (9)$$

where W_i is the weight fraction of component I, and I = 31 corresponds to the weight fraction of all components above C₃₁.

The distribution coefficients K_i of component I between the CO₂-rich phase and oil-rich phase are obtained when CO₂ and crude oil reach phase equilibrium:

$$\log K_i = -0.04175C_i + 0.7611 \quad (10)$$

where C_i is the number of carbon atoms in component I, and C₃₁₊ is replaced by the average number of carbon atoms C₃₃. If the weight fraction of the component is given in segments, the corresponding K_i can be calculated according to the average number of carbon atoms in the component.

Weight composition parameter F :

$$F = \sum_2^{31} K_i W_i \quad (11)$$

CO₂ density $\rho\rho_{mm}$ at MMP:

When $F < 1.1467$, $\rho\rho_{mm} = -0.524F + 1.189$;

When $F \geq 1.1467$, $\rho\rho_{mm} = 0.42$.

The pressure corresponding to this density of CO₂ at MMP can be calculated based on the state equation or by looking up the CO₂ temperature-pressure-density table.

3.3 State Equation Method [30]

The PR state equation was proposed by Peng et al., and has high accuracy in calculating the critical point of mixtures. Its form is as follows:

$$p = \frac{RT}{v-b} - \frac{a\alpha(T)}{v(v+b) + b(v-b)} \quad (12)$$

For the *i* component in the mixture: $a_i = \Omega_a \times \frac{R^2 T_{ci}^2}{p_{ci}}$, $\Omega_a = 0.45724$; $b_i = \Omega_b \times \frac{RT_{ci}}{p_{ci}}$, $\Omega_b = 0.07780$.

Peng et al. used Soave’s method to determine the parameter α :

$$\alpha_i(T_i, \omega_i) = [1 + m_i(1 - T_{ri}^{0.5})]^2 \tag{13}$$

where $m_i = 0.37464 + 1.5422\omega_i - 0.26992\omega_i^2$.

Substituting the state equation of a real gas $pv = z_m nRT$ into Eq. (14), the compressibility factor cubic equation can be obtained:

$$z_m^3 - (1 - B_m)z_m^2 + (A_m - 2B_m - 3B_m^2)z_m - (A_mB_m - B_m^2 - B_m^3) = 0 \tag{14}$$

where $A_m = \frac{a_m(T)p}{(RT)^2}$, $B_m = \frac{b_m p}{RT}$.

For mixtures, the following mixing rules are generally used:

$$a_m(T) = \sum_i^n \sum_j^n x_i x_j (a_i a_j \alpha_i \alpha_j)^{0.5} (1 - k_{ij}) \tag{15}$$

$$b_m = \sum_i^n x_i b_i \tag{16}$$

From Eqs. (16) and (17), the fugacity coefficient of the *i* component can be derived as Φ_i :

$$\ln \Phi_i = \ln\left(\frac{f_i}{x_i p}\right) = \frac{b_i}{b_m}(z_m - 1) - \ln(z_m - B_m) - H_i \tag{17}$$

where $H_i = \frac{A_m}{2\sqrt{2}B_m} \left(2\frac{\psi_j}{a_m} - \frac{b_j}{b_m}\right) \ln\left[\frac{z_m + (1 + \sqrt{2})B_m}{z_m + (1 - \sqrt{2})B_m}\right]$, $\psi_j = \sum_{j=1}^n x_j (a_i \alpha_i a_j \alpha_j)^{0.5} (1 - k_{ij})$.

3.4 Numerical Simulation Method

To determine MMP using the numerical simulation method, it is necessary to establish a numerical simulation model based on a good fit of the PVT properties of the reservoir fluids. The actual data from the reservoir is used to establish a numerical simulation model of the slim tube experiment, with injection and production wells set at the two ends of the model. The inflow and outflow of CO₂ and crude oil at different pressures are simulated, and MMP is determined by plotting the relationship between recovery rate and displacement pressure [31–33].

The numerical simulation method is a relatively mature method for determining MMP and has a wide range of applications. Currently, reservoir simulation software such as Eclipse and CMG can be used for this purpose. However, the accuracy of the calculation is greatly affected by the precision of the experiment and the selection of data.

4 Field Application and Effect

This paper investigated a total of 33 low-permeability oilfields that have implemented CO₂ EOR technology, extracting their geological characteristics and relevant parameters of field application effectiveness, as shown in Appendix and Fig. 4, and summarized them as follows.

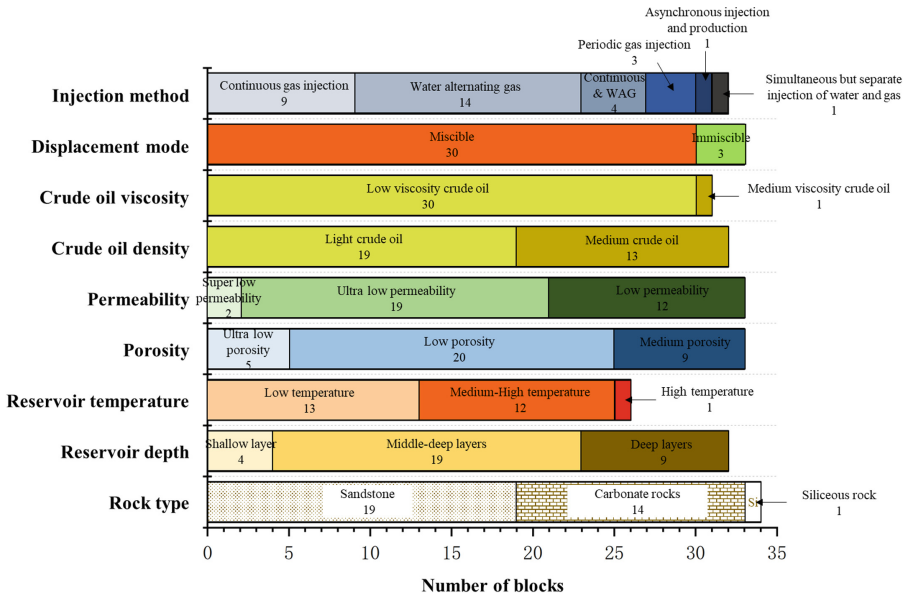


Fig. 4. Statistical Chart of the Number of Different Classified Blocks in Low Permeability Oil Reservoirs Driven by CO₂ at Home and Abroad

4.1 Lithology

Different sedimentary environments of oil reservoirs lead to different lithologies. The internal mineral composition and structure of reservoirs with different lithologies are also different, resulting in varying properties of the oil reservoirs and influencing the choice of development methods.

The surveyed blocks mainly contain Sandstone, carbonate, and siliceous rock reservoirs. Among them, there are 19 Sandstone reservoirs, accounting for 57.6%, including 16 mixed-phase reservoirs and 3 non-mixed-phase reservoirs; 14 carbonate reservoirs, accounting for 42.4%, are all mixed-phase reservoirs; and 1 siliceous rock reservoir, accounting for 3%, is a mixed-phase reservoir. The average daily oil production of Sandstone, carbonate, and siliceous rock reservoirs are 6.376t, 7.02t, and 3.02t, respectively. The CO₂ displacement effect is better in carbonate reservoirs.

4.2 Reservoir Depth and Temperature

The depth of the reservoir affects the temperature and pressure of the reservoir to a certain extent, thereby affecting the CO₂ displacement effect. When the depth of the reservoir is high, the temperature of the reservoir also increases, which can easily lead to excessively high mixed-phase pressure and difficulty in forming a mixed-phase; when the depth of the reservoir is low, the pressure of the reservoir is also low, and it is also difficult to form a mixed-phase. Nevertheless, because the mixed-phase displacement effect is better than non-mixed-phase displacement, some reservoirs will take corresponding measures to increase the formation pressure before starting CO₂ displacement to achieve mixed-phase displacement. The surveyed blocks are mostly medium-deep reservoirs in terms of depth and low- to medium-high temperature reservoirs according to temperature classification.

The lowest depth of the reservoir is 394.4 m, the highest is 3200 m, and the average depth is 1960.6 m. Among them, there are 4 shallow reservoirs (≤ 1220 m), accounting for 12.12%, all of which are mixed-phase reservoirs; 19 medium-deep reservoirs (1220–2440 m), accounting for 57.58%, including 16 mixed-phase reservoirs and 3 non-mixed-phase reservoirs; and 9 deep reservoirs (> 2440 m), accounting for 27.27%, are all mixed-phase reservoirs. The average daily oil production of single wells in medium-deep and deep reservoirs is 5.1 t and 14.575 t, respectively, and the CO₂ displacement effect is better in deep reservoirs.

The lowest temperature of the reservoir is 22.8 °C, the highest is 126 °C, and the average temperature is 71.6 °C. Among them, there are 13 low-temperature reservoirs (≤ 60 °C), accounting for 39.39%, including 12 mixed-phase reservoirs and 1 non-mixed-phase reservoir; 12 medium-high temperature reservoirs (60–120 °C), accounting for 36.36%, including 10 mixed-phase reservoirs and 1 non-mixed-phase reservoir; and 1 high-temperature reservoir (> 120 °C), accounting for 3.03%, is a mixed-phase reservoir. The average daily oil production of single wells in low-temperature and medium-high temperature reservoirs is 4.44 t and 7.88 t, respectively, and the CO₂ displacement effect is better in medium-high temperature reservoirs.

4.3 Porosity and Permeability

Porosity and permeability of reservoirs are important parameters for evaluating the storage capacity and permeability characteristics of reservoirs [34], and are also two important factors that affect the selection of development methods. Low porosity and permeability of reservoirs can lead to poor oil flowability, and conventional displacement agents may have difficulty achieving ideal results. However, supercritical CO₂, due to its strong permeability, can easily enter the tiny pores of reservoirs and displace oil more effectively. The surveyed blocks are mostly characterized by ultra-low porosity and permeability reservoirs.

The minimum porosity of the reservoir is 6%, the maximum is 23.4%, and the average porosity is 13.3%. Among them, there are 5 ultra-low porosity reservoirs ($\leq 10\%$), accounting for 15.15%; 20 low-porosity reservoirs (10–15%), accounting for 60.61%; and 8 medium-porosity reservoirs (15–25%), accounting for 24.24%. The daily production of a single well for ultra-low porosity, low porosity, and medium porosity reservoirs

is 10.88 t, 4.89 t, and 3.57 t, respectively. The CO₂ displacement effect in ultra-low porosity reservoirs is better.

The minimum permeability of the reservoir is 0.27 mD, the maximum is 46 mD, and the average permeability is 11.16 mD. There are 2 ultra-low permeability reservoirs (0.1–1 mD), accounting for 6.06%; 19 special low-permeability reservoirs (1–10 mD), accounting for 57.58%; and 12 low-permeability reservoirs, accounting for 36.36%. The daily production of a single well for ultra-low permeability and low permeability reservoirs is 3.26t and 10.96t, respectively. The CO₂ displacement effect in low-permeability reservoirs is better.

4.4 Crude Oil Density and Viscosity

Most of the low-permeability reservoirs for CO₂ displacement both domestically and abroad are light crude oil reservoirs, with a relative density ranging from 0.725 to 0.881, and an average relative density of 0.828. Among them, there are 19 light crude oil reservoirs (≤ 0.852), accounting for 57.58%; and 13 medium crude oil reservoirs (0.852–0.930), accounting for 39.39%. The daily production of a single well for light crude oil and medium crude oil reservoirs is 8.51 t and 5.39 t, respectively. Light crude oil reservoirs have a better CO₂ displacement effect.

Classified by crude oil viscosity, most of them are low viscosity oil reservoirs, with crude oil viscosity ranging from 0.2 mPa·s to 12.8 mPa·s, and an average crude oil viscosity of 2.1 mPa·s. Among them, there are 30 low viscosity oil reservoirs (≤ 10 mPa·s), accounting for 90.91%, and 1 medium viscosity oil reservoir (10–100 mPa·s), accounting for 3.03%.

4.5 Displacement Mode

There are mainly two types of CO₂ displacement modes that increase the recovery rate, namely, CO₂ miscible flooding and non-miscible flooding (see Sect. 2.4 for more details on miscible effect). For low-permeability reservoirs with CO₂ flooding in China and abroad, the miscible flooding mode is mainly used, with 30 reservoirs accounting for 90.91% and 3 non-miscible flooding reservoirs accounting for 9.09%.

CO₂ miscible flooding reservoirs are covered by Sandstone, carbonate rock, and siliceous rock. The depth of the reservoir is about 394.4–3200 m, with an average depth of 1966.3 m. The reservoir temperature is about 22.8–126 °C, with an average temperature of 70.4 °C. The porosity is about 6–23.4%, with an average porosity of 13.4%. The permeability is about 0.27–46 mD, with an average permeability of 12.1 mD. The relative density of crude oil is 0.725–0.881, with an average relative density of 0.828. The viscosity of crude oil is 0.2–12.8 mPa·s, with an average viscosity of 2.05 mPa·s.

The non-miscible CO₂ flooding reservoirs are all Sandstone reservoirs, with a concentration of depths in the middle and deep layers, about 1617–2100 m, with an average depth of 1905.7 m. The reservoirs are low-porosity and ultra-low-permeability reservoirs, with porosity of 10–12.8% and permeability of 1.16–1.9 mD. The distribution of reservoir temperature, crude oil relative density, and viscosity is similar to that of the miscible CO₂ flooding reservoirs. The temperature is 44–108 °C, the crude oil is light,

with a relative density of about 0.79–0.86, and the crude oil is low viscosity, with a viscosity of 1.91–3.6 mPa·s.

The single-well daily oil production of CO₂ miscible flooding reservoirs and non-miscible flooding reservoirs are 7.42 t and 1.025 t, respectively, with the miscible flooding effect being much better than that of non-miscible flooding.

4.6 Injection Method

The injection methods that improve the recovery rate of CO₂ flooding mainly include continuous gas injection, water-gas alternating injection, periodic gas injection, etc.

Continuous gas injection refers to the direct injection of continuous CO₂ gas into the formation. This method has a fast effect and high oil recovery efficiency, but the consumption of CO₂ is large, and early gas channeling is prone to occur, with a small affected area and rapid gas production increase [17].

Water-gas alternating (WAG) injection is a method of driving oil by alternately injecting CO₂ and water into the reservoir with smaller segment plug sizes. Although injection of water may cause water blockage and CO₂ to bypass crude oil [17], this method can effectively improve the problem of early gas channeling during continuous gas injection. Injecting CO₂ into the reservoir reduces the viscosity of crude oil and expands its volume, which is beneficial to expanding the affected area and improving oil recovery efficiency [18].

Periodic injection involves injecting a cycle of CO₂ into a formation, followed by shutting the well for a period of time before injecting the next cycle. This method has the advantages of continuous injection, alternating between water and gas, and CO₂ sequestration. During the shut-in period, CO₂ comes into contact with the crude oil, reducing its viscosity and increasing its volume, thereby improving oil recovery through the mechanism of CO₂ EOR. However, this method requires a long time due to the need to shut-in the well [35].

In addition, some oil fields have developed their own targeted CO₂ EOR models based on their specific conditions. For example, the Hua 26 block in the Subei Basin uses an asynchronous injection and production method, while the Weyburn oil field in Canada uses a method of injecting water and gas separately but simultaneously [36, 37].

Of the surveyed blocks, 9 blocks, accounting for 27.27%, used continuous injection and all were using miscible flooding; 14 blocks, accounting for 42.42%, used alternating injection of water and gas, with one block being a non-miscible reservoir; 4 blocks, accounting for 12.12%, started with continuous injection and then switched to alternating injection or used both injection methods simultaneously, with one block being a non-miscible reservoir; 3 blocks, accounting for 9.09%, used periodic injection, with one block being a non-miscible reservoir; and there were 1 block each for asynchronous injection and separate injection of water and gas, both accounting for 3.03%, and both using miscible flooding. Among them, the periodic injection method had a daily oil production rate of 13.64 t per well, far better than other injection methods.

5 Conclusion and Outlook

- (1) CO₂-EOR technology achieves its oil recovery purpose mainly through the changes in reservoir rock and fluid properties, gas dissolution drive and miscibility effects. The minimum miscibility pressure (MMP) of CO₂ and crude oil can be obtained through experimental methods, empirical formulae, equation of state, and numerical simulation methods. Among them, the experimental method yields more accurate results, the empirical formula and equation of state methods are more convenient, and the numerical simulation method has a wide range of applications, but the results are greatly affected by the original data.
- (2) The application of CO₂-EOR technology in low-permeability reservoirs is mainly concentrated in the following types of reservoirs: classified by reservoir depth, mainly in middle and deep reservoirs; classified by reservoir temperature, mainly in low-temperature and medium-to-high-temperature reservoirs; classified by pore structure, mainly in ultra-low porosity and ultra-low permeability reservoirs; classified by crude oil properties, mainly in light crude oil reservoirs and low-viscosity crude oil reservoirs. The displacement mode tends to be miscible displacement, and the CO₂ injection methods are mainly water alternating gas injection and continuous injection.
- (3) In the oil fields where CO₂ is currently used to improve oil recovery, carbonate reservoirs have better displacement effects than other rock types; deep, medium-to-high temperature, ultra-low porosity, low-permeability, and light crude oil reservoirs have better displacement effects than other reservoir properties; in terms of displacement and injection methods, miscible displacement and cyclic injection have better effects than other methods.
- (4) CO₂-EOR can not only significantly increase the recovery rate of low-permeability reservoirs, but also achieve effective CO₂ sequestration, which is of great significance to ensure national energy security and achieve the carbon peaking and carbon neutrality goals, and has broad application prospects. However, attention should also be paid to balancing the increase in recovery rate and geological sequestration, so as to achieve a more secure and economically benign promotion.

Appendix

See Table 1.

Table 1. Table of Specific Parameters for CO₂-EOR of Low Permeability Reservoirs at Home and Abroad

No.	Block	Rock type	Reservoir depth (m)	Reservoir temperature (°C)	Porosity (%)	Permeability (mD)	Relative density of crude oil	Crude oil viscosity (mPa.s)	Injection start time	Injection method	Miscible or not	Statistics Time for Recovery Efficiency	Single well daily oil production (t)	Cumulative incremental oil (10 ⁴)	Reference
Mend-															
1	Strawn Field, Texas, USA	Sandstone	1363.98	57.22	9.4	12	0.82	1.3	1964	Continuous gas injection	Yes			[38]-[39]	
2	Levelland Field, Texas, USA	Dolomitic limestone	1493.52		10.2	2.1	0.876	1.9	1972	Continuous gas injection	Yes	2014	2.36	[9],[40][42]	
3	the SACROC Unit of the Kelly-Snyder Field, Texas, USA	Dolomite	2043.5	54	9.41	19.4	0.82	0.35	1972	Water alternating gas	Yes	2014	9.7	[8]-[9],[37][38][40]	
4	Twofreds (Delaware) Field Unit, Texas, USA	Sandstone	816.8	28.3	20.3	27.7	0.825	1.4	1974	Water alternating gas	Yes			[40][43]	
5	Little Creek Field, Mississippi, USA	Sandstone	3170	120	23.4	33	0.825	0.4	1974	Water alternating gas	Yes	2014	3.57	[9],[37],[43][44]	
6	Slaughter Estate Unit(SEU), Texas, USA	Dolomite	1519	40.6	12	4.9	0.865	2	1976	Water alternating gas	Yes	2014	1.61	[9],[38][43][45][46]	
7	Granny's Creek Field, West Virginia, USA	Sandstone	609.6		16	7	0.799	1.94	1976	Water alternating gas	Yes			[47]	
8	Hilly Upland Field	Dolomite	394.4	25	14	3	0.816	1.7	1976	Water alternating gas	Yes			[43],[48]	
9	Rock Creek Field, West Virginia, USA	Sandstone	601.9	22.8	21.7	21.5	0.811	3.2	1979	Water alternating gas	Yes			[49]	

(continued)

Table 1. (continued)

10	Little Knife Field, North Dakota, USA	Dolomitized carbonate rock	3000	118.33	18	22	0.82	0.2	1981	Water alternating gas	Yes	[40],[50]
11	Purdy Springer NE, Oklahoma, USA	Sandstone	2286	64.44	13	44	0.835	1.41	1982	Continuous gas injection , Water alternating gas	Yes	[51],[52]
12	Wasson(Dever Unit), Texas, USA	Dolomite	1584.96	40.55	12	5	0.86	1.1	1983	Continuous gas injection , Water alternating gas	Yes	2014 3.31 [9],[40],[53]
13	Maljamar Field, New Mexico, USA	Dolomitic sandstone, Dolomite	1230	32.22	11	18	0.865	1	1983	Continuous gas injection	Yes	[40],[55]
14	South Pine Field	Crystalline dolomite	2800	105	19	20			1983	Water alternating gas	Yes	[43]
15	Hamford, Texas, USA	Limestone	1676.4		10.5	4.01	0.865	1.38	1984	Water alternating gas	Yes	[40],[55]
16	Vacuum, New Mexico, USA	Dolomite	1341.12	38.33	11.7	11	0.835	1	1985	Water alternating gas	Yes	[40],[56]
17	Devonian Unit, Texas, USA	Flint	2377	48.9	13.5	9	0.825	0.4	1985	Continuous gas injection	Yes	2014 3.02 [9],[40],[43],[57]
18	S. Wasson Clearfork, Texas, USA	Dolomite	2100		6	2	0.865		1986	Water alternating gas	Yes	2014 6.53 [9],[58]

(continued)

Table 1. (continued)

19	Rangely Weber, Colorado, USA	Sandstone	1827	71.1	12	10	0.849	2	1986	Yes	2014	0.68	[9],[59]
20	Midale, Saskatchewan, CAN	Limestone, Dolomite	1402.08		13	15	0.865	3	1986	Yes	2014	19.6	[9],[60][61]
21	Slaughter Sundown(SS U), Texas, USA	Marine carbonate	1524	41.7	12	3	0.865		1994	Yes	2014	3.26	[9],[37][40]
22	Weyburn Field, CAN	Dolomite, Dolomite Limestone	1500	60	11	7	0.881	3	2000	Yes	2014	9.8	[9],[37]
23	Caoshe Oilfield, North Jiangsu Basin, CHN	Sandstone	3020	119	14.8	46	0.879	12.8	2005	Yes	2020	13.52	[62][63][64]
24	Shu 101, Yushulin Oilfield, CHN	Sandstone	2000	108	10	1.16	0.855	3.6	2007	No	2022	1.7	[65][66]
25	Daqingzi Jing-Jilin Oilfield, CHN	Siltstone	2350	97.3	10.4	2.86	0.779	3.75	2008	Yes	2021	32	[67][70]
26	Gao 89-1 Block, Shengli Oilfield, CHN	Limé, Argillaceous , Dolomitic siltstone	2900	126	12.5	4.7	0.738	1.59	2008	Yes	2021	8.6	[62][71]- [73]

(continued)

Table 1. (continued)

27	Yaojingtai Oilfield, CHN	Sandstone	2100	90	12.1	1.9	0.79	1.91	2011	Continuous gas injection, Water alternating gas	No	2019	1.74	[62],[74]-[76]
28	Qiaojawa Oilfield, CHN	Sandstone	1617	44	12.8	1.2	0.86	2.5	2012	Water alternating gas	No	2019	0.35	0.18062 [77]-[79]
29	Fan 142-7-X4, Shengli Oilfield, CHN	Sandstone	3000		12.5	1.2	0.746	1.18	2013	Periodic gas injection	Yes	2021	1.4	[73],[80]
30	Wuqi Oilfield, CHN	Sandstone			12.8	0.783	0.782	2.38	2014	Continuous gas injection	Yes	2020	1.23	[77],[81]
31	Zhangjiaduo Oilfield, CHN	Sandstone	3200	112	17	5	0.8	1.74	2015	Continuous gas injection	Yes	2019	1.93	[62],[82]
32	Chang 8 in Huang 3 District, Changqing Oilfield, CHN	Fine sandstone, Fine-Medium sandstone, Siltstone - Fine sandstone	2750	85	8.3	0.27	0.725	1.81	2017	Periodic gas injection	Yes	2018	25.58	0.1532 [83]-[86]
33	Hua 26 Block, North Jiangsu Basin, CHN	Sandstone	3140	112	15.7	2.6	0.87	2.41	2017	Asynchronous injection and production	Yes	2021	0.83445	

References

1. Tang, W., Zhang, G., Xu, P.: Analyze key areas and orientations of technological innovation for oil and gas exploration and development in 14th five-year plan period. *Pet. Sci. Technol. Forum* **41**(5), 7–15 (2022)
2. U.S Energy Information Administration: Technically recoverable shale oil and shale gas resources: an assessment of 137 shale formations in 41 countries outside the United States. U.S Energy Information Administration, 10 June 2013
3. Wang, C., Hong, L., Gao, R., et al.: Status-quo and challenges of enhanced oil recovery in low permeability reservoirs. *Unconventional Oil Gas* **5**(3), 102–108 (2018)
4. Wenrui, H.: The present and future of low permeability oil and gas in China. *Strateg. Study CAE* **11**(8), 29–37 (2009)
5. Wang, Z., Cao, G., Bai, Y., et al.: Development status and prospect of EOR technology in low- permeability reservoirs. *Special Oil Gas Reservoirs*, 1–17 (2023)
6. Ding, S., Xi, Y., Liu, G., et al.: Adaptability of different injection methods of CO₂ flooding in low permeability reservoirs to enhanced oil recovery and geological storage. *Petrol. Geol. Recovery Effic.* **30**, 1–8 (2023)
7. Wang, X., Yang, H., Wang W., et al.: Technology and practice of CO₂ flooding and storage in low-permeability tight reservoirs. *Petrol. Geol. Recovery Effic.*, 1–9 (2023)
8. Qin, J., Han, H., Liu, X.: Application and enlightenment of carbon dioxide flooding in the United States of America. *Pet. Explor. Dev.* **42**(2), 209–216 (2015)
9. Koottungal, L.: 2014 worldwide EOR survey. *Oil Gas J.* **112**(4), 79–91 (2014)
10. Yuan, S., Wang, Q., Li, J., et al.: Technology progress and prospects of enhanced oil recovery by gas injection. *Acta Petrolei Sinica* **41**(12), 1623–1632 (2020)
11. Song, X., Wang, F., Ma, D., et al.: Progress and prospect of carbon dioxide capture, utilization and storage in CNPC oilfields. *Pet. Explor. Dev.* **50**(1), 206–218 (2023)
12. Li, S., Tang, Y., Hou, C.: Present situation and development trend of CO₂ injection enhanced oil recovery technology. *Petrol. Reservoir Eval. Dev.* **9**(03) (2019)
13. Gao, H., He, Y., Zhou, X.: Research progress on CO₂ EOR technology. *Special Oil Gas Reservoirs* **16**(1), 6–12, 106 (2009)
14. Jia, W., Song, S., Li, C., et al.: Progress of oily sludge extraction by supercritical CO₂. *Chem. Ind. Eng. Progress* **41**(12) (2022)
15. Wang, X.: CO₂ Flooding Technology in Low Permeability Sandstone Reservoir. Petroleum Industry Press, Beijing (2017)
16. Gu, L., Li, Z., Ou, J.: The existing state of enhanced oil recovery by utilizing carbon dioxide. *China Min. Mag.* **10**, 66–69 (2007)
17. Zhu, C, Cheng, L.: Reserch on CO₂ flooding in low permeability reservoir. *Drill. Prod. Technol.* **30**(6), 55–57, 60, 144–145 (2007)
18. Jia, K., Ji, D., Gao, J., et al.: The existing state of enhanced oil recovery by CO₂ flooding in low permeability reservoirs. *Unconventional Oil Gas* **6**(1), 107–114, 61 (2019)
19. Cheng, S., Liu, S., Zhu, S.: The mechanism and popularization application of single well CO₂ huff and puff for increasing oil production. *Oil-Gas Field Surface Eng.* **10**, 16–17 (2003)
20. Dai, B., Wang, L., Zhuang, J.: Experiment of minimum miscible pressure of CO₂ flooding in ultra-low permeability reservoir. *Lithologic Reservoirs* **32**(2), 129–133 (2020)
21. Fang, Z.: Calculation of Minimum Miscibility Pressure for CO₂-Hydrocarbon System. China University of Petroleum, Beijing (2019)
22. Liang, M., Yuan, H., Yang, Y., et al.: Research progress on miscible gas displacement and determination of minimum miscibility pressure. *J. Southwest Petrol. Univ. (Sci. Technol. Edn.)* **39**(5), 101–112 (2017)

23. Wang, Q.: Review on determine methods of minimum miscibility phase pressure of CO₂ miscible flooding. *Chem. Ind. Eng. Progress* **30**(S1), 805–808 (2011)
24. Huang, C., Tang, R., Yu, H., et al.: Determination of the minimum miscibility pressure of CO₂ and crude oil system by hanging drop method. *Lithologic Reservoirs* **27**(1), 127–130 (2015)
25. Yellig, W.F., Metcalfe, R.S.: Determination and prediction of CO₂ minimum miscibility pressures (includes associated paper 8876). *J. Petrol. Technol.* **32**(01), 160–168 (1980)
26. Glaso, O.: Generalized minimum miscibility pressure correlation. *SPE J.* (12), 927934 (1985)
27. Alston, R.B., Kokolis, G.P., James, C.F.: CO₂ minimum miscibility pressure: a correlation for impure CO₂ streams and live oil systems. *SPE J.* **25**(2), 268–274 (1985)
28. Silva, M.K., Orr, F.M., Jr.: Effect of oil composition on minimum miscibility pressure - part 1: solubility of hydrocarbons in dense carbon dioxide. *SPE Reservoir Eng.* **2** (1987)
29. Yang, X.: Study on the Minimum Miscibility Pressure of Gas Injection in Oil Reservoirs. Southwest Petroleum University, Chengdu (2003)
30. Ye, A., Guo, P., Wang, S., et al.: Determination of minimum miscibility pressure for CO₂ flooding by using PR equation of state. *Lithologic Reservoirs* **24**(6), 125–128 (2012)
31. Gao, Z.: The Production Technology by Injecting Gas of Oil Field. Petroleum Industry Press, Beijing (1994)
32. Hao, Y., Chen, Y., Yu, H.: Determination and prediction of minimum miscibility pressure in CO₂ flooding. *Petrol. Geol. Recovery Effic.* (6), 64–66, 87 (2005)
33. Zhang, G., Li, Z., Liu, J., et al.: Study on determine methods of minimum miscibility pressure of hydrocarbon injection miscible flooding. *Drill. Prod. Technol.* **144**(03), 99–102+157 (2008)
34. Lu, P.: Research on Porosity and Permeability Model of Tight Sandstone Reservoirs Based on Machine Learning-Taking the Eight Member of the Shihezi Formation of the Upper Paleozoic in the Middle Part of the Western Margin of the Ordos Basin as an Example. Northwest University, Xi'an (2022)
35. He, Y., Zhou, X., Li, M., et al.: Injection mode of CO₂ displacement in extra-low permeability reservoirs. *J. Oil Gas Technol.* **32**(06), 131–134+531 (2010)
36. Li, Y., Huang, W., Jin, Y., et al.: Different reservoir types of CO₂ flooding in Sinopec EOR technology development and application under “dual carbon” vision. *Petrol. Reservoir Eval. Dev.* **11**(6), 793–804, 790 (2021)
37. Shen, P., Liao, W.: Geological Storage of Carbon Dioxide and Technology for Improving Oil Recovery. Petroleum Industry Press, Beijing (2009)
38. Klins, M.A.: Carbon Dioxide Flooding Mechanism and Engineering Design. Shaojin, C. (Trans.). Petroleum Industry Press, Beijing (1989)
39. Holm, L.W., O'Brien, L.J.: Carbon dioxide test at the Mead-Strawn field. *J. Pet. Technol.* **23**, 431–442 (1971)
40. Manrique, E.J., Muci, V.E., Gurfinkel, M.E.: EOR field experiences in carbonate reservoirs in the United States. *SPE Res. Eval. Eng.* **10**, 667–686 (2007)
41. Graham, B.D., Bowen, J.F.: Design and implementation of a Levelland unit CO₂ Tertiary pilot. SPE 8831, Tulsa (1980)
42. Brannan, G., Whittington, H.M.: Enriched Gas Miscible Flooding: A Case History of the Levelland Unit Secondary Miscible Project, SPE 5826, IOR. Tulsa, OK (1976)
43. Liu, Y., Liu, J., et al.: Polymer and Carbon Dioxide Oil Displacement Technology. China Petrochemical Press, Beijing (2001)
44. Youngren, G.K., Charlson, G.S.: History match analysis of the little creek CO₂ pilot test. *J. Pet. Technol.* **32**, 2042–2052 (1980)
45. Merchant, D.H., Thakur, S.C.: Reservoir management in tertiary CO₂ floods. Paper presented at the SPE Annual Technical Conference and Exhibition, Houston, Texas, October 1993
46. Stein, M.H., Frey, D.D., Walker, R.D., Pariani, G.J.: Slaughter estate unit CO₂ flood: comparison between pilot and field-scale performance. *J. Pet. Technol.* **44**, 1026–1032 (1992)

47. Watts, R.J., Conner, W.D., Wasson, J.A., Yost, A.B.: CO₂ injection for tertiary oil recovery, Granny's creek field, Clay county, West Virginia. Paper presented at the SPE Enhanced Oil Recovery Symposium, Tulsa, Oklahoma, April 1982
48. Watts, R.J., Gehr, J.B., Wasson, J.A., Evans, D.M., Locke, C.D.: A single CO₂ injection well minitest in a low-permeability carbonate reservoir. *J. Pet. Technol.* **34**, 1781–1788 (1982)
49. Brummert, A.C., Watts, R.J., Boone, D.A., Wasson, J.A.: Rock creek oil field CO₂, pilot tests, Roane County, West Virginia. *J. Pet. Technol.* **40**, 339–347 (1988)
50. Desch, J.B., Larsen, W.K., Lindsay, R.F., Nettle, R.L.: Enhanced oil recovery by CO₂ miscible displacement in tie little knife field, Billings County, North Dakota. In: SPE 10696, 3rd EOR, Tulsa (1982)
51. Fox, M.J., Simlote, V.N., Beaty, W.G.: Evaluation of CO₂ flood performance, Springer 'A' Sand, NE Purdy Unit, Garvin County, Oklahoma. Paper SPE 12665 presented at the 1984 SPE/DOE Enhanced Oil Recovery Symposium, Tulsa, Oklahoma, 15–16 April (1984)
52. Fox, M.J., Simlote, V.N., Stark, K.L., et al.: Review of CO₂ flood, Springer "A" sand, Northeast Purdy Unit, Garvin County, Oklahoma. *SPE Reserv. Eng.* **3**(4), 1161–1167 (1988)
53. Tanner, C.S., Baxley, P.T., Crump, J.G., et al.: Production performance of the Wasson Denver unit CO₂ flood. In: Society of Petroleum Engineers. Society of Petroleum Engineers (1992)
54. Pittaway, K.R., Albright, J.C., Hoover, J.W., et al.: The Maljamar CO₂ pilot: review and results. *J. Petrol. Technol.* **39**(10), 1256–1260 (1987)
55. Merritt, M.B., Groce, J.F.: A case history of the Hanford San Andres Miscible CO₂ project. *J. Petrol. Technol.* **44**(08), 924–929 (1992)
56. Brownlee, M.H., Sugg, L.A.: East vacuum Grayburg-SanAndres Unit CO₂ injection project: development and results to date. In: SPE 16721, 62nd ATCE, Dallas (1987)
57. Poole, E.S.: Evaluation and implementation of CO₂ injection at the Dollarhide Devonian Unit (1988)
58. Burbank, D.E.: Early CO₂ flood experience at the South Wasson Clearfork unit. In: SPE/DOE Enhanced Oil Recovery Symposium (1992)
59. Fullbright, G.D., Hild, G.P., Korf, T.A., et al.: Evolution of conformance improvement efforts in a major CO₂ WAG injection project. In: SPE/DOE Improved Oil Recovery Symposium. Society of Petroleum Engineers (1996)
60. Beliveau, D., Payne, D.A., Mundry, M.: Waterflood and CO₂ flood of the fractured Midale field (includes associated paper 22947). *J. Petrol. Technol.* **45**(09), 881–887 (1993)
61. Beliveau, D.A.: Midale CO flood pilot. *J. Can. Petrol. Technol.* **26**(06) (1987)
62. Ji, B., He, Y.: Practice and understanding about CO₂ flooding in low permeability oil reservoirs by Sinopec. *Petrol. Reservoir Eval. Dev.* **11**(6), 805–811, 844, 790 (2021)
63. Zhang, F., Wang, Z.: The field experiment and results analysis of CO₂ miscible displacement in Caoshe oilfield of the north Jiangsu Basin. *Pet. Geol. Exp.* **32**(3), 296–300 (2010)
64. Zhang, Y.: CO₂-EOR and Geological Storage Study of Jiangsu Caoshe Oil-Field. China University of Petroleum (East China), Qingdao (2010)
65. Song, Y.: Evaluation of Oil Displacement Effect by CO₂ Flooding of FUYANG Reservoirs in DAQING Oilfield. China University of Petroleum, Beijing (2016)
66. Zhang, Y., Yang, T., Yang, Z., et al.: Evaluation of oil displacement by CO₂ at Fuyang extra-low permeability layer in Yushulin oilfield. *Sci. Technol. Rev.* **33**(5), 52–56 (2015)
67. Yuan, S., Ma, D., Li, J., et al.: Progress and prospects of carbon dioxide capture, EOR-utilization and storage industrialization. *Pet. Explor. Dev.* **49**(4), 828–834 (2022)
68. Hu, Y., Hao, M., Chen, G., et al.: Technologies and practice of CO₂ flooding and sequestration in China. *Pet. Explor. Dev.* **46**(4), 716–727 (2019)
69. Zhang, X., Kou, G., Wang, Z., et al.: Technical discussion on development effects of CO₂ flooding in Jilin extra-low permeability reservoir. *Drill. Prod. Technol.* **42**(2), 64–67, 4–5 (2019)

70. Guofeng, W.: Carbon dioxide capture, enhanced-oil recovery and storage technology and engineering practice in Jilin Oilfield, NE China. *Pet. Explor. Dev.* **50**(1), 219–226 (2023)
71. Cao, X., Lyu, G., Wang, J., et al.: Technology and application of CO₂ flooding in ultra-low permeability beach-bar sand reservoir. *Petrol. Reservoir Eval. Dev.* **9**(3), 41–46 (2019)
72. Li, C.: Application of CO₂ miscible flooding technology in the development of ultra-low permeability reservoirs in Block Gao 89-1. *J. Oil Gas Technol.* **33**(06), 328–329 (2011)
73. Zhang, Z., Lyu, G., Wang, J.: CCUS and its application in Shengli Oilfield. *Petrol. Reservoir Eval. Dev.* **11**(06), 812–822+790 (2021)
74. Wang, J., Gao, Y., Zong, C., et al.: Response characteristics of CO₂-immiscible-flooding wag in the ultra-low permeability oil reservoirs. *Petrol. Geol. Oilfield Dev. Daqing* **35**(02), 116–120 (2016)
75. Liao, H.: Numerical simulation of oil displacement with carbon dioxide in DB34 well block, Yaoyingtai Oilfield. *J. Xi'an Shiyou Univ. (Nat. Sci. Edn.)* **25**(05), 50–53+109 (2010)
76. Dong, C., Gao, Z., Li, X.: Pilot study on CO₂ displacement in Yaoyingtai Oilfield. *Liaoning Chem. Ind.* **47**(06), 578–579+582 (2018)
77. Kang, Y., Bai, Y., Jiang, S., et al.: Technical features and engineering practice of Yanchang full-chain carbon capture, utilization and storage project. *Appl. Chem. Ind.* **49**(7), 1768–1771, 1775 (2020)
78. Wang, Y., Li, W., Jia, Z., et al.: The development practice and effect analysis for CO₂ injection in Chang 6 reservoir of Qiaojiawa Oilfield. *Unconventional Oil Gas* **3**(03), 75–79 (2016)
79. Yang, H., Jiang, S., Wang, H., et al.: Research of adaptability of gas channeling controlling methods in CO₂ flooding of fractured ultra- low permeability reservoir. *J. Xi'an Shiyou Univ. (Nat. Sci. Edn.)* **32**(02), 105–109+115 (2017)
80. Yang, Y.: Research and application of CO₂ flooding technology in extra-low permeability reservoirs of Shengli oilfield. *Petrol. Geol. Recovery Effic.* **27**(1), 11–19 (2020)
81. Qi, C., Li, R., Zhu, S., et al.: Pilot test on CO₂ flooding of Chang 4+51 oil reservoir in Yougou region of the Ordos Basin. *Oil Drill. Prod. Technol.* **41**(2), 249–253 (2019)
82. Ren, B.: Analysis of CO₂ displacement mechanism in the third member of Fujiang formation in Zhangjiaduo oilfield. *Petrochem. Ind. Technol.* **27**(04), 97–98 (2020)
83. Li, M., Li, Y., Yang, J., et al.: Research and on-site testing of CO₂ flooding technology in Huang 3 district. *Petrochem. Ind. Appl.* **39**(5), 71–75 (2020)
84. Li, K., Lo, P., Wei, M., et al.: A pilot project of CO₂ enhanced oil recovery and storage in Chang 8 extra-low permeability reservoir in Huang 3 district of Changqing oilfield. *J. Eng. Geol.* **29**(5), 1488–1496 (2021)
85. Tang, Y., Liao, S., Lei, X., et al.: Study on improving the sweep efficiency of CO₂ flooding in low permeability fractured reservoirs in Huang-3 block. *Petrol. Reservoir Eval. Dev.* **9**(03), 9–13 (2019)
86. Wang, S., Ma, G., Lang, Q., et al.: Study on formation mechanism and prevention technology of gas channeling by CO₂ flooding in low permeability fractured reservoirs. *Energy Chem. Ind.* **43**(03), 29–34 (2022)